Brief Communication

MOLECULAR METABOLISM

Hypothalamic miR-219 regulates individual metabolic differences in response to diet-induced weight cycling

Mariana Schroeder [1,2,**,3], **Yonat Drori** [1,2,3], **Yair J. Ben-Efraim** [1,2], **Alon Chen** [1,2,*]

ABSTRACT

Consumption of a low calorie diet is the most common approach to lose weight. While generally effective at first, it is frequently followed by a relapse where the pre-diet weight is regained, and often exceeded. This pattern of repeated weight loss/regain is referred to as weight cycling and the resulting metabolic response varies greatly between individuals.

Objective: We attempted to address the issue of individual differences in the response to weight cycling in male mice.

Methods: We first exposed adult wild type mice to repeated cycles of high/low fat food. Next, using a lentiviral approach, we knocked-down or over-expressed miR-219 in the ventromedial hypothalamus (VMH) of an additional mouse cohort and performed a full metabolic assessment.

Results: Exposure of wild type males to weight cycling resulted in the division of the cohort into subsets of resistant versus metabolic-syndrome-prone (MS) animals, which differed in their metabolic profile and hypothalamic miR-219 levels. Lentiviral knock-down of miR-219 in the VMH led to exacerbation of metabolic syndrome. In contrast, over-expression of miR-219 resulted in moderation of the metabolic syndrome phenotype.

Conclusions: Our results suggest a role for miR-219 in the mediation of the metabolic phenotype resulting from repeated weight cycling.

Keywords Weight cycling; Metabolic syndrome; miRNAs; Ventromedial hypothalamus; High fat diet; Diabetes

1. INTRODUCTION

The growing and worldwide obesity epidemic is suggested to be the result of the conceptual gap between the environmental conditions in which our metabolic regulatory systems evolved and the environment that we live in today. Thus, an individual living in an environment with a limited food supply that requires intense physical activity would benefit from the consumption of energy dense food and high metabolic efficiency. Conversely, the present lifestyle in the Western world offers excessive amounts of (high fat) food and lower physical activity levels and represents a challenge for the maintenance of normal energy balance and therefore results in high rates of overweight and obesity [1]. To date, dieting is the cornerstone approach in obesity management. However, maintaining the reduced body weight following a diet period remains a great challenge for most individuals. Thus, following initial weight loss, weight is gradually regained often beyond the pre-diet weight, raising concerns about subsequent long-term, adverse health consequences resulting from repeated dieting. This pattern of repeated weight loss and regain is a phenomenon referred to as weight cycling (WC) or "yo-yo dieting" [2,3]. WC often results in an overall gain rather than loss of weight in the long-term due to the body's natural tendency to regain lost weight [4,5]. While initially predominantly linked to weight gain, WC has more recently been implicated in increased risk for eating disorders and metabolic syndrome (MS). MS consists of a clustering of medical conditions that include visceral fat accumulation, high blood pressure, dyslipidemia, glucose intolerance, and insulin resistance, all of which represent a serious risk to health. Despite the similar end point body weight between obese individuals that have experienced WC and individuals with chronic obesity, different mechanisms may be involved in these two distinct patterns of weight gain [6]. Of particular interest is the mechanism underlying the different responses to WC among individuals with a similar genetic/environmental background.

The hypothalamus, and especially the medio-basal hypothalamus, is the key brain region that integrates peripheral and central signals relaying information on the nutritional state and the changing energy

[1]Department of Neurobiology, Weizmann Institute of Science, Rehovot, 76100, Israel [2]Department of Stress Neurobiology and Neurogenetics, Max-Planck Institute of Psychiatry, Munich, 80804, Germany

[3] Equal contribution.

*Corresponding author. Department of Neurobiology, Weizmann Institute of Science, Rehovot, 76100, Israel. Fax: +972 8 9344131. E-mails: alon.chen@weizmann.ac.il, alon_chen@psych.mpg.de (A. Chen).

**Corresponding author. Department of Stress Neurobiology and Neurogenetics, Max-Planck Institute of Psychiatry, Munich, 80804, Germany. E-mail: schatzyo@gmail.com (M. Schroeder).

Received August 28, 2017 • Revision received January 10, 2018 • Accepted January 18, 2018 • Available online 2 February 2018

https://doi.org/10.1016/j.molmet.2018.01.015

requirements, thus maintaining constant energy homeostasis. The ventromedial hypothalamus (VMH) contains neurons that directly respond to glucose and is involved in hepatic glucose metabolism by efferent sympathetic nervous system fibers that reach the liver via the splanchnic nerve [7]. A new, additional level of complexity to the mechanism of metabolic balance has emerged with the newly found hypothalamic small noncoding RNAs (miRNAs) involvement in the regulation of energy homeostasis, including metabolism related processes such as insulin secretion, glucose and lipid metabolism (reviewed in [8]), and metabolic response to high fat diet (HFD) feeding or caloric restriction [9].

In the present study, we examined the individual differences in the metabolic profile of mice subjected to repeated metabolic challenge in parallel to the hypothalamic miRNA footprint with the objective of exploring the central molecular mechanisms responsible for the individual differences in the metabolic response to WC. We report that repeated WC selectively induced weight gain, glucose intolerance, insulin resistance, and hyper-adiposity in a subset of mice in a manner similar to chronic HFD exposure but did not have any long-lasting effects on a further subset of genetically identical animals. Our results suggest that miR-219 in the VMH plays a central role in the mediation of energy homeostasis. We discovered that by knocking down miR-219 in the VMH, the predisposition to metabolic disease increased significantly. In contrast, when overexpressed, miR-219 in the VHM moderately protected the animals from this phenotype. We have therefore exposed a potential miRNA mediated hypothalamic mechanism involved in coping with WC that result in susceptibility or resistance to metabolic disease.

2. MATERIALS AND METHODS

2.1. Animals

Male C57BL/6J mice (IMSR_JAX:000664) and pregnant female ICR mice and their pups (IMSR_JAX:009122) were maintained in a pathogen-free temperature-controlled (22 $\pm$ 1 °C) mouse facility on a reverse 12 h light/dark cycle at the Weizmann Institute of Science, according to institutional guidelines. Food and water were given *ad libitum*.

2.2. Weight cycling model

In order to establish a model of repetitive weight gain and loss, 9-week-old C57BL/6J male mice (n = 60) were fed *ad libitum* HFD (60% of calories) (D12492 Research Diets Inc., New Brunswick, NJ, USA) for 3 weeks followed by 2 weeks of *ad libitum* regular chow diet (Harlan Biotech Israel Ltd, Rehovot, Israel). This procedure was repeated 3 consecutive times (a total of 15 weeks). Mice were weighed twice a week. This cycling period was chosen following a preliminary experiment showing that the change in weight gain following 3 weeks of HFD and 2 weeks of regular chow is relatively moderate. Following the WC protocol, the metabolic phenotype of the mice was evaluated by determining whole-body glucose homeostasis, indirect calorimetry, and body composition.

2.3. Glucose and insulin tolerance tests

Glucose (2 g/kg body weight) was injected i.p. following 6.5 h of fasting. Whole venous blood obtained from the tail vein at 0, 15, 30, 60, 90, and 120 min after the injection was measured for glucose using an automatic glucometer (Roche). For the insulin tolerance test, mice were injected with insulin (0.75 or 1 units/kg body weight) following 4–5 h of fasting. Blood glucose levels were measured 0, 15, 30, 60, and 90 min after insulin injection.

2.4. Body composition

Body composition was assessed using the EchoMRI-100TM (Echo Medical Systems, Houston, TX, USA).

2.5. Metabolic studies

Indirect calorimetry, food, and water intake, as well as locomotor activity were measured using the LabMaster system (TSE-Systems, Bad Homburg, Germany). The LabMaster instrument consists of a combination of feeding and drinking sensors for automated online measurement. The calorimetry system is an open-circuit system that determines O_2 consumption, CO_2 production, and respiratory exchange ratio. A photobeam-based activity monitoring system detects and records ambulatory movements, including rearing and climbing, in every cage. All of the parameters are measured continuously and simultaneously. Data were collected after a 24 h adaptation period in acclimated, single housing.

2.6. Hypothalamic mRNA extraction and miRNAs expression profile

At the end point of the WC experiment, fresh hypothalami were collected and snap frozen on dry ice. Total mRNA was isolated using miRNeasy mini kit (QIAGEN, Hilden, Germany), and commercially profiled with the nCounter miRNA Expression Assay (Nanostring Technologies, Seattle, WA). Raw data were normalized to positive control counts and to the 100 most abundantly expressed miRNAs, and adjusted for background corrections using nCounter Data Analysis.

2.7. Cloning of 3′ UTRs into Psicheck2 luciferase expression plasmid

3′UTR sequence of Cnrip1 was PCR amplified from mouse genomic DNA using the following primers: 5′-ATGATTCCTTCTGATGTTGC-3′ and 5′-ATTACCATTCCATACACGGT-3′. 3′UTR fragment was then ligated into pGem-T easy vector (Promega, Madison, WI) according to the manufacturer's guidelines, and 15 further subcloned into a single NotI site at the 3′ end of luciferase in the Psicheck2 reporter plasmid (Promega, Madison, WI). Cloning orientation was verified by diagnostic cuts and sequencing. A mutated form of Cnrip1 3′UTR lacking all 6 bases of miR-219 conserved seed-match sequence was established by generating 2 partially complementary PCR fragments, used as templates for ligation PCR (primers: 5′-CTGATGTTGCAACTCCAGAAA-3′ and 5′-CAGTTTCTGGAGTTGCAACAT-3′, each used with 1 of the aforementioned primers). The 3′UTR sequences of Cc2d1a and Rbms1 were sub-cloned as described above using the following primers — Cc2d1a 3′UTR: 5′-CCCATCCTGGACTACAGGC-3′ and 5′-GCCTTGGCTGTTCATTCTGT-3′; Cc2d1a mutated 3′ UTR: 5′-CAACTGTCCGCTGCTTGTCTGTT-3′ and 5′-ACAGACAAGCAGCGGACAGTTGG-3′; Rbms1 3′UTR: 5′-CTGTGAGATGTACCGAAGGG-3′ and 5′-TGTTAGTGTACAGCCTTATAAACA-3′; Rbms1 mutated 3′UTR: 5′-GAAGGCTGATGGATTTTTC-3′ and 5′-AAAATCCATCAGCCTTCAC-3′.

2.8. Transfections and luciferase assay

Huh7 cells were grown on poly-L-lysine-coated 48-well plates to a 70–85% confluence and transfected using jetPEI (Polyplus-transfection SA, Illkirch, France) according to manufacturer's instructions with the following plasmids: 5 ng of Psicheck2-3′ UTR plasmid and 215 ng of enhanced green fluorescent protein (EGFP) overexpressing vector for either miR-219, or a scrambled-miR EGFP plasmid. Forty-eight hours following transfection, cells were lysed, and luciferase reporter activity was assayed as previously described [10]. Renilla luciferase values were normalized by control luciferase levels (transcribed from the same vector but not affected by the 3′ UTR tested) and averaged across 8 well repetitions per condition.

2.9. Design, construction, and validation of miR-219 lentiviruses

The miR-219 overexpression vector was cloned as follows: the enhanced form of human synapsin I promoter [11] was PCR amplified (F: TTTTTTATCGATCTCGAGTAGTTA TTAATAGTAATC; R: TTTTTTACC-GGTGGCGCGCCCGCCGCAGCGCAGATGGT) from pENTR1A-E/SYN-GFP-WRPE1 (kindly provided by Dr Takeshi Kaneko, Department of Morphological Brain Science, Graduate School of Medicine, Kyoto University, Kyoto, Japan) and inserted between ClaI and AgeI restriction sites to replace the CMV promoter in pCSC-SP-PW-GFP (kindly provided by Dr Inder Verma, The Salk Institute for Biological Studies, La Jolla, CA). Following the synapsin promoter, the precursor for miR-219 was inserted as follows: ATCTGGTGTCCCCGCTTCCGCGCGGCGTCTC-TATCCCCGGTGCCTCCGATGCGCTTCTCTCCCCGTCCCGGGCCGCGGCTC-CTGATTGTCCAAACGCAATTCTCGAGTCTCTGGCTCCGGCCGAGAGTTGC-GTCTGGACGTCCCGAGCCGCCGCCCCCAAACCTCGAGGGGGAGAGGCCG-GGCGGAGCGCGGGACGGTCCCCGGACACCCGGGACCCCGCCGCAGCCCT-AGGATCTCAGGGCGCGCACCCAGCAGCAGAGGTGCAGCT. A control scramble sequence was purchased from GeneCopoeia and was similarly inserted into the same plasmid as the miR-219 precursor sequence. The H1-miR-219 knockdown (KD) and its control scramble sequence were obtained from GeneCopoeia and subcloned into the NheI site of the p156RRL-CMV-GFP viral plasmid. High titer lentiviruses were produced as described previously [12]. Briefly, recombinant lentiviruses were produced by transient transfection in HEK293T cells. Infectious particles were harvested at 48 and 72 h post-transfection, filtered through 0.45 μm-pore cellulose acetate filters, concentrated by ultracentrifugation, re-dissolved in sterile HBSS, aliquoted and stored at −80 °C.

2.10. Stereotactic intracranial injections

The lentiviruses were injected using a computer-guided stereotaxic instrument and a motorized nanoinjector (Angle Two Stereotaxic Instrument, myNeurolab, Leica Biosystems, Buffalo Grove, IL). Mice were anesthetized using 1.5% isoflurane and 1 μl of the lentiviral preparation was delivered to each VMH using a Hamilton syringe connected to a motorized nanoinjector system at a rate of 0.15 μl per minute (coordinates relative to bregma: AP = −1.46 mm, ML = ±0.3 mm, DV = −5.5 mm). Mice were subjected to the WC protocol 1 week following injection.

2.11. *In situ* hybridization for miR-219 detection

Paraffin sections of adult C57BL/6 brains (−1.58 mm from bregma) were hybridized with DIG-labeled locked nucleic acid (LNA) probes (Exiqon, Vedbaek, Denmark) overnight at 55 °C (U6 and miR-219) and 60 °C (miR-124) as previously described in [13] and developed with nitro blue tetrazolium chloride/5-Bromo-4-chloro-3-indolyl phosphate (NBT/BCIP) medium.

2.12. Real time PCR analysis

Quantitative expression of the following genes was acquired and analyzed using a step 1 thermocycler (Applied Biosystems, Waltham, MA), using primers that were designed specifically for them.

MiR-219-5p: 5′- TGATTGTCCAAACGCAATTCT - 3′.
Cnrip1: 5′- TAAAGAGCCTGACGGGGAGA - 3′ and 5′- CCACACTGT-CTCGAAGGTCC - 3′
Cc2d1a: 5′- ACCCTCTACCAGTCTGCACT - 3′ and 5′- AGCAGGT-TTTCCAGCGTCTT - 3′
Htr1a: 5′- GTGCACCATCAGCAAGGACC - 3′ and 5′- GCGCCGAA-AGTGGAGTAGAT - 3′
Rbms1: 5′- TACGTGATTCCAGTGGTGCC - 3′ and 5′- ACTCCTGG-TGGGGTCTTGAT - 3′
Sarcolipin: 5′- TGTGCCCCTGCTCCTCTTC - 3′ and 5′- TGATTGCA-CACCAAGGCTTG - 3′

RNA samples were assessed using miScript Reverse transcription kit and SYBRGreen PCR kit (QIAGEN, Hilden, Germany) according to the manufacturer's guidelines. U6 snRNA was used as the internal control.

2.13. Western blot analysis

Hypothalami from a separate set of WC animals were homogenized in RIPA buffer and incubated on ice for 10 min. Homogenate was centrifuged for 15 min and supernatant was transferred into a new tube, and samples were added with sample buffer and boiled for 5 min. Samples were separated on a 12% acrylamide gel SDS PAGE and transferred to a nitrocellulose membrane. Following blocking with 10% milk, αCnrip1 (rabbit polyclonal anti-CNRIP1, AB_10709018), αCc2d1a (rabbit monoclonal anti-Cc2d1a ab191472, abcam, Cambridge, UK), and αActin (mouse monoclonal anti-actin, Cell Signaling Technology, Beverly, MA) were added overnight at 4 °C. Secondary antibodies were added at room temperature for 2 h (anti-rabbit HRP and anti-mouse HRP, Cell Signaling Technology, Beverly, MA). Finally, ECL was added to the membrane, which was exposed to film.

2.14. Statistical approach

The allocation of each WC animal into the resistant, moderate, and MS-prone subgroups was determined by Hierarchical cluster analysis using the Ward method and squared Euclidean distance. The strength of the predictors was determined by Two-step clustering. The different MS parameters were analyzed using parametric tests, T-tests, ANOVA, and repeated measures ANOVA when relevant. To compare between the WC, KD, and OE experiments, Z scores of the injected treatment groups (miR-219 KD/OE) were first normalized to the scramble controls within each experiment, and then each score was multiplied by the predictors' score in the WC experiment. To gain statistical power and visualize the effect the miRNA manipulations had on their global scores, the scramble groups were next divided into two new subgroups. Those with positive Z scores were defined as MS-prone and those with negative scores were defined as resistant. The miR-219 KD and miR-219 OE global scores and average raw data were then compared to the different scramble subgroups to get an estimation of their position in the response-spectrum. All data were analyzed using IBM SPSS version 20 and Graphpad Prism5.

3. RESULTS

To mimic human WC in mice, we established a mouse model using alternating diets of regular chow and HFD as previously described [3,14,15]. Two variations of WC animal models have been reported: 1) Models applying the use of limited access to HFD in order to induce weight gain (e.g. [3,14,15]), and models applying the use of a low fat diet for the induction of weight loss (e.g. [6,16]. Here, we applied a variation of the first approach on 60 male C57BL/6J mice. Mice were subjected to 3 consecutive feeding cycles, each cycle consisting of 3 weeks of HFD feeding and 2 weeks of chow feeding *ad libitum*. When the alternating diet cycles ended, mice were fed only with regular chow (Figure 1A). Two age-matched control groups were fed *ad libitum* regular chow or HFD for the same time period. Body weight was continuously monitored and following 2 weeks of chow access at the end of the 15-week WC protocol, glucose and insulin tolerance,

MOLECULAR METABOLISM

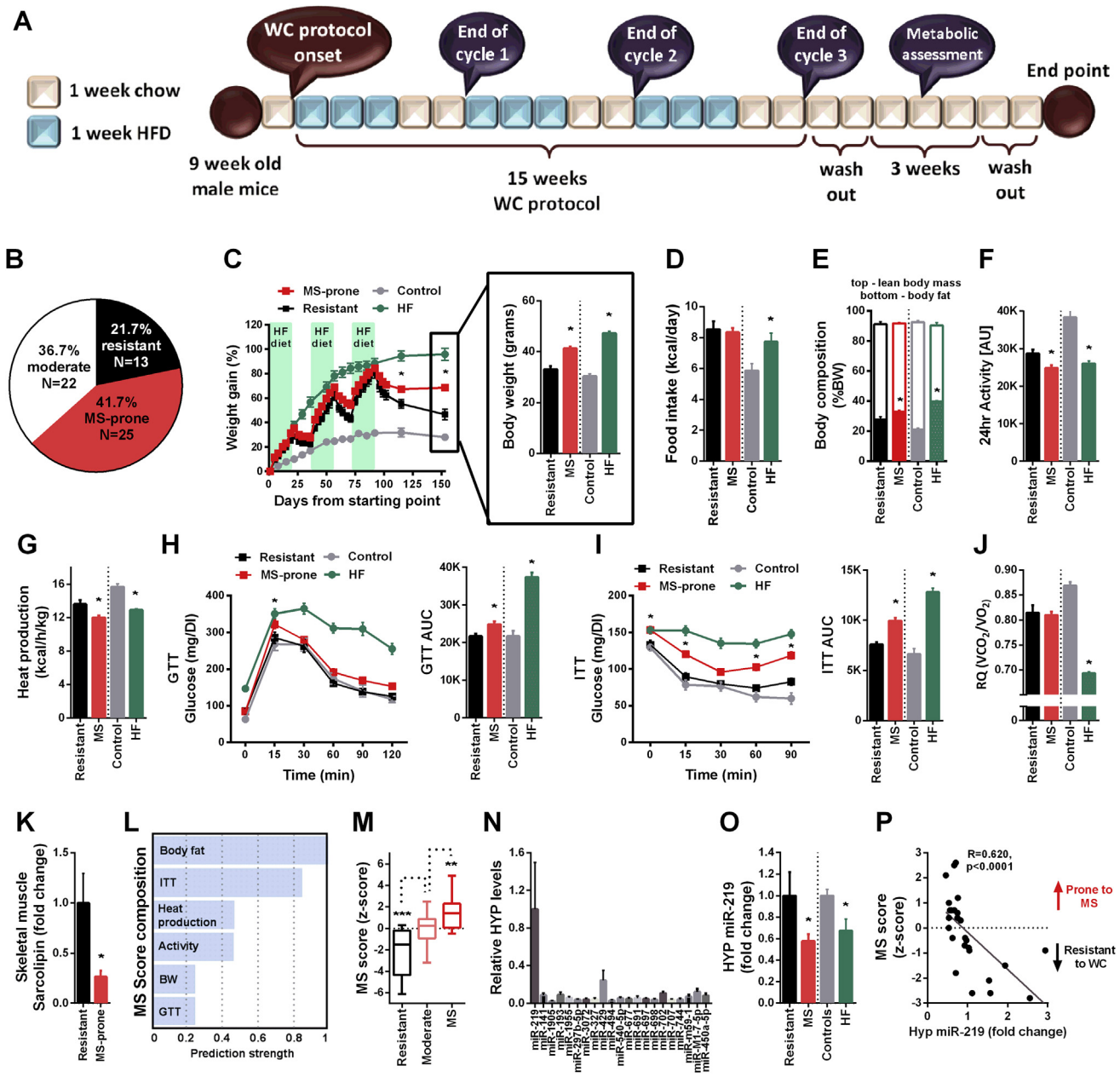

Figure 1: Repeated weight cycling results in different metabolic phenotypes according to hypothalamic expression of miR-219. (A) Schematic representation of the experimental design for the weight cycling (WC) protocol. **(B)** Cluster analysis revealed 3 response sub-groups (metabolic syndrome prone (MS), moderate, and resistant) among adult mice. Multivariate analysis of variance showed a significant difference between the MS-prone, resistant, high fat and control animals in the 8 parameters examined ($F_{(24,192)} = 13.59$, $p = 0.000$). **(C)** Body weight change differed between "MS" and resistant ($F_{int(31,1116)} = 4.68$, $p = 0.013$). End point BW was higher in MS-prone and HF groups ($F_{(3,73)} = 71.95$, $p = 0.000$). **(D)** Food intake was similar between resistant, MS animals and HF animals and was higher than controls ($F_{(3,73)} = 5.02$, $p = 0.003$). **(E)** Body fat was higher in MS animals compared to resistant and similar to animals on chronic HFD ($F_{(3,73)} = 63.33$, $p = 0.000$). **(F)** 24hr activity ($F_{(3,73)} = 30.51$, $p = 0.000$) and **(G)** heat production ($F_{(3,73)} = 28.82$, $p = 0.000$) were lower in MS animals and similar to the HFD group. **(H)** Glucose tolerance was impaired in MS animals ($F_{main(1,34)} = 6.39$, $p = 0.016$), as reflected by the increased AUC ($t_{(36)} = 2.65$, $p = 0.012$). **(I)** A similar pattern of disrupted insulin tolerance was found in MS animals ($F_{main(1,35)} = 31.09$, $p = 0.000$), as reflected by the increased AUC ($t_{(36)} = 5.37$, $p = 0.000$). **(J)** The respiratory quotient (RQ) was similar between resistant and MS animals and was in-between the control and HF groups ($F_{(3,73)} = 95.23$, $p = 0.000$). **(K)** Skeletal muscle Sarcolipin was lower in MS-prone animals ($t_{(16)} = 2.44$, $p = 0.027$). **(L)** Prediction strength of each parameter according to the cluster analysis. Data are presented in min to max. **(M)** A metabolic syndrome score was calculated for each animal combining all examined parameters. MS animals displayed a higher MS-score than resistant animals and moderate animals displayed a higher MS-score than resistant animals ($F_{(2,57)} = 23.64$, $p < 0.0001$). **(N)** Hypothalamic miRNA expression array exposed miR-219 as the most abundant among the miRNAs affected by WC when comparing resistant versus MS animals. **(O)** The downregulation of miR-219 in MS animals resembles the hypothalamic reduction in chronically fed HFD animals compared to controls ($t_{(19)} = 2.11$, $p = 0.048$ for resistant versus MS and $t_{(10)} = 2.63$, $p = 0.025$) for control versus HFD). Data are presented as mean and S.E.M. **(P)** The MS score calculated for each animal individually, inversely correlated with their hypothalamic expression of miR-219 ($R = 0.620$, $p < 0.0001$). $N = 26$.

metabolic rate, general activity, and body composition were assessed in all animals to evaluate their metabolic state. Using these 6 parameters, animals were split into either "metabolic syndrome-prone (MS)," "resistant," or "moderate" by cluster analysis. Accordingly, most of the animals presented a MS (42%) or moderate (37%) phenotype, while only 22% were resistant to WC (Figure 1B). In order to better distinguish between the characteristics of these phenotypes, we analyzed each of the parameters separately comparing "MS" versus "resistant" animals in parallel to chow and HFD controls. MS animals gained more weight after WC and weighed significantly more than resistant animals in the end of the protocol (Figure 1C). MS animals consumed a similar number of calories (Figure 1D), gained more fat (Figure 1E), displayed lower general activity (Figure 1F) and metabolic rate (Figure 1G) and higher glucose intolerance (Figure 1H) and insulin resistance (Figure 1I) compared to resistant animals. The respiratory quotient (RQ), an indicator of the type of fuel (carbohydrate or fat) that is being metabolized to supply the body with energy, did not differ between the groups (Figure 1J). Finally, we measured the mRNA level of Sarcolipin in the gastrocnemius muscle of resistant versus MS-prone animals as a peripheral measurement of muscle-based thermogenesis [17]. MS-prone animals displayed dramatically lower levels of Sarcolipin mRNA, further predisposing MS animals to diet-induced obesity (Figure 1K). Overall, MS animals displayed a similar pathological phenotype compared to HFD controls, only more moderate. In contrast, resistant animals did not differ from chow controls and displayed complete resistance to WC, suggesting explicit individual differences in the response to the same metabolic challenge. To further confirm the individual profile of these 3 clusters, we performed a further analysis in which we attributed each individual animal a "metabolic syndrome score," composed of the sum of the Z scores of the 6 measured parameters (body fat, insulin sensitivity, heat production, activity levels, BW change, and glucose tolerance) according to their strength of prediction in the cluster analysis (for a detailed explanation see statistical analysis section). Finally, we calculated a metabolic syndrome score (MS score) for each animal combining all of the parameters measured, which revealed significant differences between resistant, moderate and MS animals (Figure 1L–M).

To elucidate the underlying mechanism responsible for these differences, we performed a miRNA array analysis from hypothalami of resistant and MS mice. A subset of 21 miRNAs were differentially expressed in "MS" mice compared to "resistant" mice (Table S1). We focused on miR-219-5p, which showed the greatest difference between the groups and was the most abundant among the chosen miRNAs (Figure 1N). Similarly to the difference between controls on chow and HFD, MS mice presented significantly lower expression of hypothalamic miR-219 (Figure 1O). The MS score of each animal was then correlated with the expression of miR-219, which revealed a significant inverse correlation between proneness to MS and hypothalamic levels of miR-219 (Figure 1P).

In order to examine the endogenous expression of miR-219 within the hypothalamus, we performed *in situ* hybridization for the detection of mature miR-219 and identified expression in the VMH and dorsomedial hypothalamus (DMH) (Figure 2A). However, miR-219 is not specific to the hypothalamus and is widely expressed in different brain areas (Figure 2B). MiR-219 is predicted to target ~300 potential transcripts (http://www.targetscan.org). After a careful literature and bioinformatic screening of these predicted targets, we chose 4 putative transcripts potentially involved in the MS phenotype: 1) cannabinoid receptor interacting protein 1 (*Cnrip1*), 2) coiled-coil and C2 domain containing 1A (Cc2d1a), 3) RNA binding motif, single stranded interacting protein 1 (Rbms1), and 4) serotonin receptor 1A (Htr1a). The 3′UTRs of these transcripts contain 1 seed match for miR-219, which is conserved in several species, including mouse and human. However, only 2 of these 4 putative targets showed an inverse correlation with miR-219 (Figure 2C–F). We therefore focused on the potential regulatory effect of miR-219 on Cnrip1 and Cc2d1a *in vitro* using luciferase assays. Accordingly, the protein levels of both targets were significantly higher in MS WC hypothalamic samples (Figure 2G, I). Finally, luciferase gene expressing constructs fused to wild type or mutated 3′UTRs of Cnrip1 or Cc2d2a transcripts were co-transfected with miR-219 overexpressing plasmid. Both constructs' activity was significantly inhibited by miR-219 overexpression and blocked by mutation of the miR-219 seed match sequence, further validating them as targets of miR-219 (Figure 2H, J).

To explore the involvement of hypothalamic VMH/DMH miR-219 on the mouse metabolic performance, we next generated a mouse model with reduced levels of miR-219 in the VMH/DMH of adult WT mice using lentiviruses that express a miR-219 KD construct. Control animals were injected with a scrambled (SCR) control construct and both viruses also expressed GFP (Figure 3A). The miR-219 KD expressing lentiviruses were injected bilaterally into the VMH of 10-week old male C57BL/6J mice (miR-219 KD $n = 16$, control $n = 28$). The injection site was verified at the experiment endpoint resulting in the exclusion of 3 mice in the KD and 5 mice in the control group due to inaccurate site injection. Infection with miR-219 KD in the VMH expanded into the DMH (Figure 3B) and induced an efficient reduction in miR-219 levels by about ~50%. In these samples, miR-219 levels were inversely correlated with *Cnrip1* but not with *Cc2d1a* (Figure 3C). After a recovery period of 1 week, the animals' proneness to MS was tested by exposing all animals to the WC protocol (Figure 3D). We next calculated the individual MS score for each animal based on their body fat, insulin sensitivity, heat production, activity levels, BW change, and glucose tolerance, according to their strength of prediction as determined in the WC experiment (Figure 1J) and performed a cluster analysis (for a detailed explanation see statistical analysis section). MiR-219 KD duplicated the amount of MS-prone animals (Figure 3E). Specifically, the animals injected with the miR-219 KD virus showed a higher MS score than resistant but a similar score compared to MS animals injected with the scramble virus, suggesting that low levels of hypothalamic miR-219 expression lead to a MS prone phenotype after WC (Figure 3F). Accordingly, miR-219 KD animals showed higher body weight change (Figure 3G) despite similar food intake (Figure 3H), higher body fat (Figure 3I), lower activity levels (Figure 3J) and metabolic rate (Figure 3K), a higher glucose response 15 min after glucose administration (Figure 3L), and impaired insulin sensitivity compared to WC resistant animals (Figure 3M). The RQ was similar between the groups (Figure 3N). In contrast, miR-219 KD animals showed no differences when compared to MS prone animals (Figure 3G–M).

With the aim of producing animals more resistant to the negative effects of WC, we next tried the opposite approach; we generated a mouse model that overexpresses (OE) miR-219 in the VMH of adult WT mice, using lentiviruses expressing miR-219 and GFP under the neural-specific promoter synapsin (Figure 4A). The injection site was again verified at the experiment endpoint resulting in the exclusion of 4 mice in the OE and 4 mice in the control group due to inaccurate injection site. Infection with miR-219 OE in the VMH expanded, as before, into the DMH (Figure 4B) and induced an efficient increase in miR-219 levels. In these samples, miR-219 levels were inversely correlated with *Cnrip1* and *Cc2d1a* (Figure 4C). After a recovery period

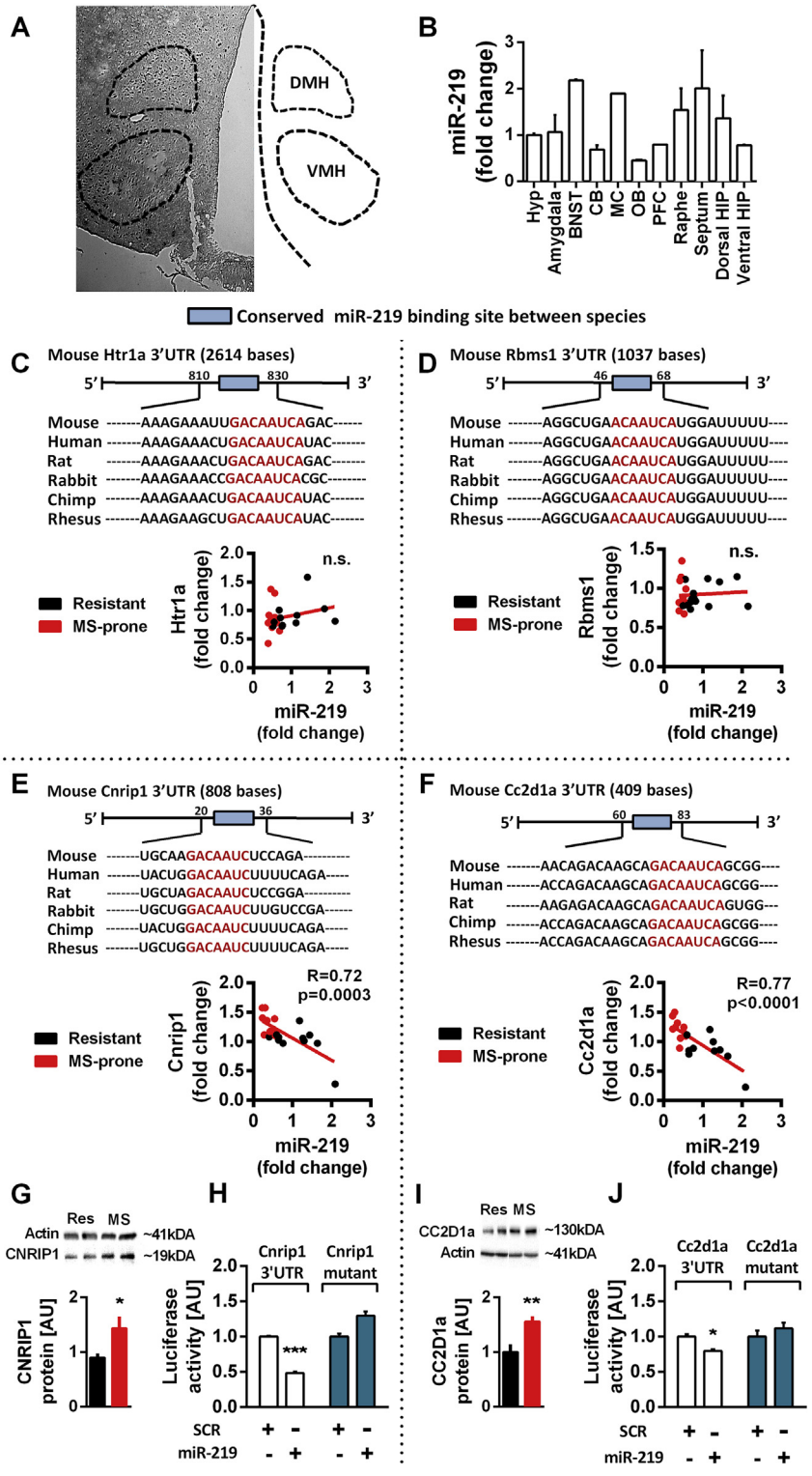

Figure 2: MiR-219 targets Cnrip1 and Cc2d1a in the hypothalamus. (A) *In situ* hybridization of miR-219 shows its expression across the ventromedial hypothalamus (VMH) and dorsomedial hypothalamus (DMH). **(B)** MiR-219 expression in different brain areas. **(C)** Schematic representation of Htr1a 3′UTR showing the putative seed match for miR-219 and seed conservation in multiple organisms. *Hrt1a* mRNA expression did not inversely correlate with miR-219. **(D)** Schematic representation of Rbms1 3′UTR showing the putative seed match for miR-219 and seed conservation in multiple organisms. *Rbms1* mRNA expression did not inversely correlate with miR-219. **(E)** Schematic representation of Cnrip1 3′UTR showing the putative seed match for miR-219 and seed conservation in multiple organisms. *Cnrip1* mRNA expression showed a significant inverse correlation with miR-219. **(F)** Schematic representation of Cc2d1a 3′UTR showing the putative seed match for miR-219 and seed conservation in multiple organisms. *Cc2d1a* mRNA expression showed a significant inverse correlation with miR-219. **(G)** CNRIP1 protein levels were elevated in MS animals ($t_{(11)} = 2.468$, $p = 0.0312$, $N = 6–7$). **(H)** *In vitro* luciferase assay assessing the effect of miR-219 on the 3′UTR of Cnrip1 further validated Cnrip1 as target, an effect that was abolished by targeted mutation of the seed ($F_{int(1,28)} = 105.9$, $p < 0.0001$). **(I)** CC2D1a protein levels were elevated in MS animals ($t_{(10)} = 3.209$, $p = 0.0094$, $N = 6$). **(J)** *In vitro* luciferase assay assessing the effect of miR-219 on the 3′UTR of Cc2d1a further validated it as target, an effect that was abolished by targeted mutation of the seed ($F_{int\ (1,28)} = 6.49$, $p = 0.017$). Data presented as mean and SEM. Hyp: Hypothalamus; CB: Cerebellum; MC: Motor cortex; OB: Olfactory bulb; PFC: Prefrontal cortex; HIP: Hippocampus.

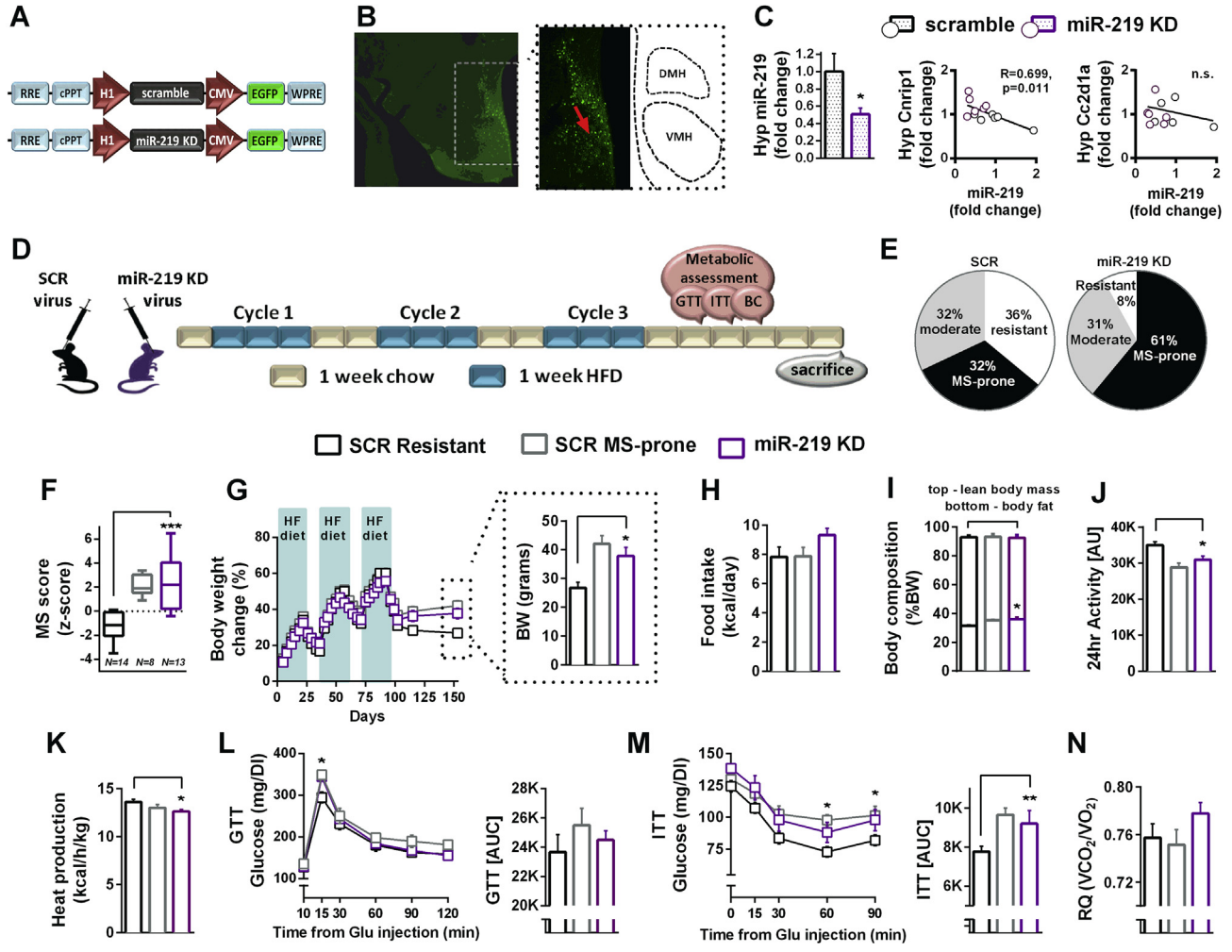

Figure 3: Hypothalamic miR-219 knockdown with lentiviral vectors leads to a metabolic syndrome-prone phenotype after weight cycling. (A) Schematic representation of miR-219 KD and control constructs under the regulation of H1 promoter. **(B)** Representative image of the injection site for the miR-219 KD expressing lentivirus (×10 magnification; red arrow). **(C)** Hypothalamic miR-219 was downregulated in miR-219 KD versus scrambled (SCR) animals ($t_{(11)} = 2.41$, $p = 0.035$, $N = 6,6$). MiR-219 expression levels inversely correlated with *Cnrip1* but not with *Cc2d1a* mRNA. **(D)** Experimental design. **(E)** Pie charts showing the distribution of each virus group among the different phenotypes. MiR-219 KD duplicated the amount of MS-prone animals. **(F)** The metabolic syndrome (MS) was calculated for each animal according to the prediction strength of each parameter in the original WC experiment. Cluster analysis of the Z scores split the animals into MS and resistant response to WC. Animals injected with the miR-219 KD virus were prone to MS as a result of the WC protocol ($F_{(2,32)} = 18.24$, $p < 0.0001$). Data presented in min. to max. **(G)** Body weight change differed between the groups ($F_{int(64,1024)} = 3.955$, $p < 0.0001$). At the end of the WC protocol, miR-219 KD animals weighed more than resistant and did not differ from MS animals ($F_{(2,32)} = 9.381$, $p < 0.0006$). **(H)** Food intake did not differ between the groups. **(I)** Body fat was higher in miR-219 KD compared to resistant animals ($F_{(2,64)} = 7.005$, $p = 0.0018$). **(J)** General activity ($F_{(2,32)} = 9.397$, $p = 0.0006$) and **(K)** Heat production ($F_{(2,32)} = 4.133$, $p = 0.0253$) were lower in miR-219 KD compared to resistant animals. **(L)** The glucose tolerance test (GTT) was similar between the groups despite a higher peak 15 min after glucose administration in miR-219 KD animals. **(M)** The insulin tolerance test (ITT) differed between miR-219 KD and resistant group at particular time-points, and the area under the curve (AUC) was higher in miR-219 KD versus resistant animals ($F_{(2,32)} = 3.946$, $p = 0.0294$). **(N)** The respiratory quotient (RQ) did not differ between the groups. Data are presented as mean and S.E.M. significance between each group based on Tukey's multiple comparison tests.

of 1 week, the animals' proneness to MS was tested by exposure to the WC protocol (Figure 4D). The individual calculation of the MS score was performed again based on the original parameters (Figure 1J). Cluster analysis revealed that miR-219 OE abolished the MS-prone group, switching them to the moderate area of the spectrum (Figure 4E). Specifically, animals injected with the miR-219 OE virus showed a lower MS score than MS but a similar score compared to resistant animals injected with the scramble virus, suggesting that high levels of hypothalamic miR-219 expression may provide some protection from a MS prone phenotype after WC (Figure 4F). Accordingly, miR-219 OE animals showed lower body weight change (Figure 4G) compared to MS animals, despite similar food intake (Figure 4H). Body fat (Figure 4I), metabolic rate (Figure 4K), glucose tolerance (Figure 4L), and RQ (Figure 4N) did not differ from either group, exposing an in-between, or moderate, phenotype. In contrast, activity levels were higher than in MS group (Figure 4J) and insulin sensitivity was significantly healthier than MS animals and not different from the resistant group (Figure 4M). Thus, miR-219 OE animal were located in the resistant part of the spectrum (Figure 4N).

Taken together, we found that miR-219 KD significantly increased the prevalence of MS compared to the WC animals, shifting the group to the MS-prone score area, suggesting this miRNA plays a critical role in determining susceptibility to MS following WC. In contrast, higher expression of VMH miR-219 correlated with higher resistance to MS in the original WC experiment and lentiviral induced OE of miR-219 shifted the animals to the MS resistant/

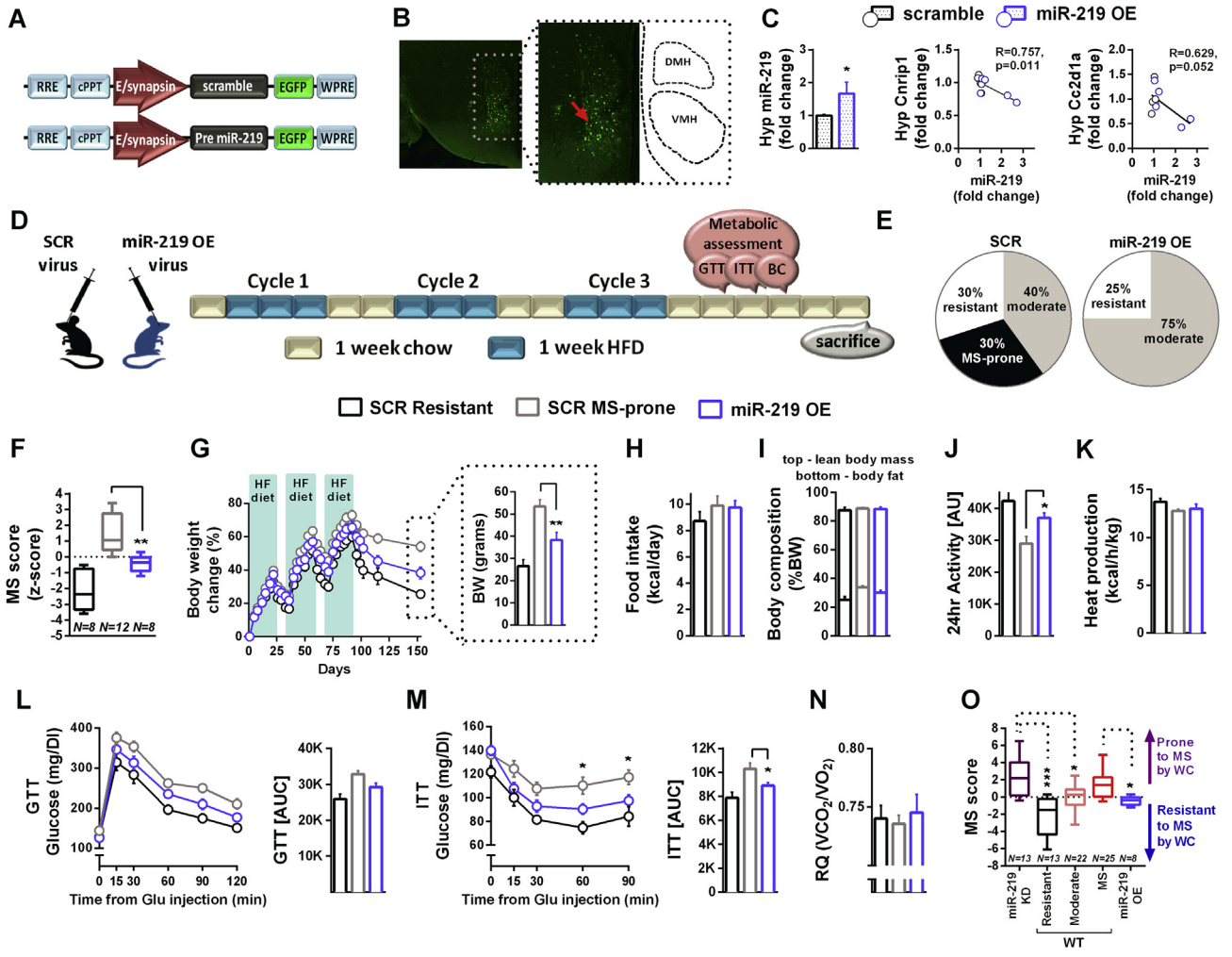

Figure 4: Hypothalamic miR-219 overexpression with lentiviral vectors protects the animals from metabolic syndrome-prone phenotype after weight cycling. (A) Schematic representation of miR-219 OE and control constructs under the regulation of E/synapsin promoter. **(B)** Representative image of the injection site for the miR-219 OE expressing lentivirus (×10 magnification; red arrow). **(C)** MiR-219 was upregulated in miR-219 OE versus scrambled (SCR) animals ($t_{(8)} = 2.71$, $p = 0.027$, $N = 5,5$). MiR-219 expression levels inversely correlated with *Cnrip1* and *Cc2d1a* mRNA. **(D)** Experimental design. **(E)** Pie charts showing the distribution of each virus group among the different phenotypes. MiR-219 OE abolished the MS-prone group. **(F)** The MS score was calculated for each animal according to the prediction strength of each parameter in the original WC experiment. Cluster analysis of the Z scores split the animals split into MS and resistant response to WC. Animals injected with the miR-219 OE virus were resistant to the WC protocol ($F_{(2,25)} = 26.49$, $p < 0.0001$) and showed significantly lower variance in their phenotype (Levene test $_{(1,26)} = 5.48$, $p = 0.027$) compared to SCR animals. Data presented min. to max. **(G)** BW change differed between the groups according to viral treatment and response to WC ($F_{int(64,800)} = 5.047$, $p < 0.0001$). At the end of the WC protocol, miR-219 OE animals weighed less than MS and did not differ from resistant animals ($F_{(2,25)} = 18.21$, $p < 0.0001$). **(H–I)** Food intake **(H)** and body fat **(I)** in miR-219 OE animals did not differ from the scramble groups. **(J)** Locomotion activity after miR-219 OE was higher than in MS and did not differ from resistant animals ($F_{(2,25)} = 9.131$, $p = 0.0011$). **(K)** Heat production did not differ between the groups. **(L)** The glucose tolerance test (GTT) differed between the groups ($F_{(2,25)} = 18.69$, $p < 0.0001$). The area under the curve (AUC) reflects the miR-219 OE animals in between both scramble groups. **(M)** The insulin tolerance test (ITT) differed between the groups ($F_{(2,25)} = 18.69$, $p < 0.0001$). The area under the curve (AUC) of the miR-219 OE group was similar to resistant and different from MS-prone animals ($F_{(2,25)} = 8.046$, $p = 0.002$). Data are presented as mean and S.E.M. **(N)** The respiratory quotient (RQ) did not differ between the groups. **(O)** The MS score was highly variable in the original (wild type - WT) WC group, which included resistant, moderate and MS animals. MiR-219 KD significantly increased the animals MS score, shifting them to the MS-prone spectrum. In contrast, miR-219 OE reduced the MS score restricting the animals to the moderate/resistant spectrum area ($F_{(4,76)} = 14.88$, $p = 0.0001$). Data are presented min to max. Significance between the groups based on Tukey's multiple comparisons test.

moderate score area, providing protection from MS (Figure 4N). In summary, our findings suggest that hypothalamic miR-219 may play an important role in the modulation of the metabolic response to repeated cycles of dieting.

4. DISCUSSION

In the present study, we have identified hypothalamic miR-219 as a candidate mediator of the individual differences in the metabolic response to repeated WC. The maintenance of energy homeostasis relies on the careful regulation between hunger/satiety and adiposity signals, which are directed at preserving a certain body weight and level of adiposity. This phenomenon complies with the "set point" theory, which proposes that perturbations in body weight lead to metabolic responses that favor returning to a previously stable weight (reviewed in [18]) through reduction in energy expenditure and increased eating behavior [18,19]. This response occurs as a result of both mild and severe weight loss both in healthy lean [20]

and obese individuals. In animal studies aimed at modeling this phenomenon, WC resulted in high adiposity [6] and hormonal and cytokine fluctuations [16,21]. However, no previous study addressed the potential mechanisms underlying the individual differences in the response to WC. Our findings were particularly striking since they show variability in the metabolic response to WC within WT male mice of a pure breed that share an identical genetic background. This suggests the involvement of epigenetic rather than genetic regulation in this process, such as prenatal factors affecting the programming of metabolic responses, as is the case for hormonal influences [22,23] and differential nutrient availability *in utero* resulting from different uterine location [24]. A number of previous studies have shown gestational programming of metabolic phenotypes in different contexts [23,25], further suggesting that susceptibility to WC may be more sensitive to maternal variables influencing the hypothalamic development and miRNA expression, than to a specific genetic background.

MiRNAs' emergence as important regulators of energy homeostasis, including insulin secretion, glucose and lipid metabolism [8] has been shown in a number of recent studies. Some examples include miR-200a, miR-200b, and miR-429, which were up-regulated in the hypothalamus of the leptin deficient ob/ob mice, and down-regulated in response to leptin treatment [26]. In that study, hypothalamic silencing of miR-200a increased the expression levels of leptin receptor and insulin receptor substrate 2, reduced mice body weight gain, and restored liver insulin responsiveness. A further study showed up-regulation of miR-383, miR-384-3p, and miR-488 in the hypothalamus of ob/ob mice [27]. Finally, infusion of oligonucleotides mimicking 10 specific miRNAs predicted to target the PI3K-Akt-mTOR pathway to the arcuate nucleus of the hypothalamus attenuated adiposity in Dicer KO [28], further implying miRNAs in the regulation of energy balance.

MiR-219 is a miRNA conserved both in human and mouse that has been previously linked to different types of cancer [29,30], neurodegeneration [31], differentiation and myelination in the CNS [32], and circadian rhythms [33]. In addition, miR-219 has emerged as an obesity specific miRNA that targets insulin signaling pathways in the amnion of obese pregnant women [34]. We found that the mechanism of action of miR-219 in modulating the response to WC probably involves, among other potential targets, the regulation of Cnrip1 and Cc2d1a. Cnrip1 encodes 2 proteins resulting from alternative splicing; CRIP1a and CRIP1b. Both proteins interact with the cannabinoid receptor type 1 (CB1). The CB1 receptor is highly expressed in the brain and has numerous functions. Specifically in the metabolic context, selective CB1 antagonism reduces food intake and induces weight loss in both humans and animals. CRIP1a acts as an endogenous inhibitor and decreases constitutive activity of the CB1 receptor [35]. Essentially, the endocannabinoid system is profoundly involved in the regulation of food intake, metabolism and energy balance [36] and has been the target of numerous pharmacotherapeutic approaches for the treatment of obesity and MS [36,37], making it a likely candidate for the regulation of the metabolic response to WC by miR-219.

Our second target, Cc2d1a (also known as Freud-1) is a transcriptional repressor for the serotonin receptor (Htr)1a, through binding to a 5′-repressor element (FRE) of the Htr1a gene [38]. CC2D1a protein is co-localized with Htr1a receptor *in vivo*, suggesting its importance in the regulation of the receptor [39]. Given the profound effects of serotonergic neurotransmission on feeding behavior, which is primarily mediated via Htr1a and Htr2c receptors [40–42], Htr1a suppression by Cc2d1a can regulate feeding behavior in response to WC. Htr1a is expressed in the VMH among other areas in the hypothalamus [40] and is therefore a likely indirect target of miR-219 through Cc2d1a regulation. Finally, a potential interaction between the serotonin and the cannabinoid systems though the Htr1a and CB1 receptors [43,44] may add a further layer of complexity to the regulation of the metabolic response to WC as a result of up/downregulation of miR-219 in the VMH.

5. CONCLUSIONS

Overall, we have identified a specific hypothalamic mechanism through which miR-219 mediates the metabolic response to WC. The endogenous variation of this miRNA in the VMH appears to determine the great variability observed in the response to a metabolic challenge among genetically identical individuals. This results in either successful or defective coping with WC that leads to the development of MS. Through targeting of Cnrip1 and Cc2d1a, we propose miR-219 as a mechanistic pathway underlying the individual response to WC.

AUTHOR CONTRIBUTIONS

M.S., Y.D., and A.C. designed the experiments. M.S. and Y.D. wrote the manuscript. Y.D. performed the manipulations and *in vitro* experiments. Y.D. and Y.B.S performed the injections. M.S. and Y.D. sacrificed the animals and collected metabolic data. A.C. supervised the project.

ACKNOWLEDGEMENTS

A.C. is the head of the Max Planck Society—Weizmann Institute of Science Laboratory for Experimental Neuropsychiatry and Behavioral Neurogenetics. This work is supported by: an FP7 Grant from the European Research Council (260463, A.C.); a research grant from the Israel Science Foundation (1565/15, A.C.); the ERANET Program, supported by the Chief Scientist Office of the Israeli Ministry of Health (3-11389, A.C.); the project was funded by the Federal Ministry of Education and Research under the funding code 01KU1501A (A.C.); research support from Roberto and Renata Ruhman (A.C.); research support from Bruno and Simone Licht; I-CORE Program of the Planning and Budgeting Committee and The Israel Science Foundation (grant no. 1916/12 to A.C.); the Nella and Leon Benoziyo Center for Neurological Diseases (A.C.); the Henry Chanoch Krenter Institute for Biomedical Imaging and Genomics (A.C.); the Perlman Family Foundation, founded by Louis L. and Anita M. Perlman (A.C.); the Adelis Foundation (A.C.); the Marc Besen and the Pratt Foundation (A.C.); and the Irving I. Moskowitz Foundation (A.C.). We thank Mr. Sharon Ovadia for his devoted assistance with animal care.

CONFLICT OF INTEREST

None.

APPENDIX A. SUPPLEMENTARY DATA

Supplementary data related to this article can be found at https://doi.org/10.1016/j.molmet.2018.01.015.

REFERENCES

[1] Berthoud, H.-R., Lenard, N.R., Shin, A.C., 2011. Food reward, hyperphagia, and obesity. American Journal of Physiology. Regulatory, Integrative and Comparative Physiology 300(6):R1266–R1277. https://doi.org/10.1152/ajpregu.00028.2011.

[2] Lu, H., Buison, A., Uhley, V., Jen, K.L., 1995. Long-term weight cycling in female Wistar rats: effects on metabolism. Obesity Research 3(6):521—530.

[3] Ernsberger, P., Koletsky, R.J., Baskin, J.S., Collins, L.A., 1996. Consequences of weight cycling in obese spontaneously hypertensive rats. The American Journal of Physiology 270(4 Pt 2):R864—R872.

[4] van Dale, D., Saris, W.H., 1989. Repetitive weight loss and weight regain: effects on weight reduction, resting metabolic rate, and lipolytic activity before and after exercise and/or diet treatment. The American Journal of Clinical Nutrition 49(3):409—416.

[5] Prentice, A.M., Jebb, S.A., Goldberg, G.R., Coward, W.A., Murgatroyd, P.R., Poppitt, S.D., et al., 1992. Effects of weight cycling on body composition. The American Journal of Clinical Nutrition 56(1 Suppl):209S—216S.

[6] Dankel, S.N., Degerud, E.M., Borkowski, K., Fjære, E., Midtbø, L.K., Haugen, C., et al., 2014. Weight cycling promotes fat gain and altered clock gene expression in adipose tissue in C57BL/6J mice. American Journal of Physiology. Endocrinology and Metabolism 306(2):E210—E224. https://doi.org/10.1152/ajpendo.00188.2013.

[7] Szabo, A.J., Iguchi, A., Burleson, P.D., Szabo, O., 1983. Vagotomy or atropine blocks hypoglycemic effect of insulin injected into ventromedial hypothalamic nucleus. The American Journal of Physiology 244(5):E467—E471.

[8] Dumortier, O., Hinault, C., Van Obberghen, E., 2013. MicroRNAs and metabolism crosstalk in energy homeostasis. Cell Metabolism 18(3):312—324. https://doi.org/10.1016/j.cmet.2013.06.004.

[9] Sangiao-Alvarellos, S., Pena-Bello, L., Manfredi-Lozano, M., Tena-Sempere, M., Cordido, F., 2014. Perturbation of hypothalamic microRNA expression patterns in male rats after metabolic distress: impact of obesity and conditions of negative energy balance. Endocrinology 155(5):1838—1850. https://doi.org/10.1210/en.2013-1770.

[10] Chen, A., Perrin, M., Brar, B., Li, C., Jamieson, P., Digruccio, M., et al., 2005. Mouse corticotropin-releasing factor receptor type 2alpha gene: isolation, distribution, pharmacological characterization and regulation by stress and glucocorticoids. Molecular Endocrinology (Baltimore, Md.) 19(2):441—458. https://doi.org/10.1210/me.2004-0300.

[11] Hioki, H., Kameda, H., Nakamura, H., Okunomiya, T., Ohira, K., Nakamura, K., et al., 2007. Efficient gene transduction of neurons by lentivirus with enhanced neuron-specific promoters. Gene Therapy 14(11):872—882. https://doi.org/10.1038/sj.gt.3302924.

[12] Tiscornia, G., Singer, O., Verma, I.M., 2006. Production and purification of lentiviral vectors. Nature Protocols 1(1):241—245. https://doi.org/10.1038/nprot.2006.37.

[13] Pena, J.T.G., Sohn-Lee, C., Rouhanifard, S.H., Ludwig, J., Hafner, M., Mihailovic, A., et al., 2009. miRNA in situ hybridization in formaldehyde and EDC-fixed tissues. Nature Methods 6(2):139—141. https://doi.org/10.1038/nmeth.1294.

[14] Graham, B., Chang, S., Lin, D., Yakubu, F., Hill, J.O., 1990. Effect of weight cycling on susceptibility to dietary obesity. The American Journal of Physiology 259(6 Pt 2):R1096—R1102.

[15] Gray, D.S., Fisler, J.S., Bray, G.A., 1988. Effects of repeated weight loss and regain on body composition in obese rats. The American Journal of Clinical Nutrition 47(3):393—399.

[16] List, E.O., Berryman, D.E., Wright-Piekarski, J., Jara, A., Funk, K., Kopchick, J.J., 2013. The effects of weight cycling on lifespan in male C57BL/6J mice. International Journal of Obesity (2005) 37(8):1088—1094. https://doi.org/10.1038/ijo.2012.203.

[17] Bal, N.C., Maurya, S.K., Sopariwala, D.H., Sahoo, S.K., Gupta, S.C., Shaikh, S.A., et al., 2012. Sarcolipin is a newly identified regulator of muscle-based thermogenesis in mammals. Nature Medicine 18(10):1575—1579. https://doi.org/10.1038/nm.2897.

[18] Ravussin, Y., Leibel, R.L., Ferrante, A.W., 2014. A missing link in body weight homeostasis: the catabolic signal of the overfed state. Cell Metabolism 20(4):565—572. https://doi.org/10.1016/j.cmet.2014.09.002.

[19] Leibel, R.L., Rosenbaum, M., Hirsch, J., 1995. Changes in energy expenditure resulting from altered body weight. The New England Journal of Medicine 332(10):621—628. https://doi.org/10.1056/NEJM199503093321001.

[20] Kajioka, T., Tsuzuku, S., Shimokata, H., Sato, Y., 2002. Effects of intentional weight cycling on non-obese young women. Metabolism 51(2):149—154. https://doi.org/10.1053/meta.2002.29976.

[21] Barbosa-da-Silva, S., Fraulob-Aquino, J.C., Lopes, J.R., Mandarim-de-Lacerda, C.A., Aguila, M.B., 2012. Weight cycling enhances adipose tissue inflammatory responses in male mice. PLoS One 7(7):e39837. https://doi.org/10.1371/journal.pone.0039837.

[22] Noroozzadeh, M., Ramezani Tehrani, F., Sedaghat, K., Godini, A., Azizi, F., 2015. The impact of prenatal exposure to a single dose of testosterone on insulin resistance, glucose tolerance and lipid profile of female rat's offspring in adulthood. Journal of Endocrinological Investigation 38(5):489—495. https://doi.org/10.1007/s40618-014-0198-y.

[23] Lazic, M., Aird, F., Levine, J.E., Dunaif, A., 2011. Prenatal androgen treatment alters body composition and glucose homeostasis in male rats. The Journal of Endocrinology 208(3):293—300. https://doi.org/10.1677/JOE-10-0263.

[24] Raz, T., Avni, R., Addadi, Y., Cohen, Y., Jaffa, A.J., Hemmings, B., et al., 2012. The hemodynamic basis for positional- and inter-fetal dependent effects in dual arterial supply of mouse pregnancies. PLoS One 7(12):e52273. https://doi.org/10.1371/journal.pone.0052273.

[25] Pankevich, D.E., Mueller, B.R., Brockel, B., Bale, T.L., 2009. Prenatal stress programming of offspring feeding behavior and energy balance begins early in pregnancy. Physiology & Behavior 98(1—2):94—102. https://doi.org/10.1016/j.physbeh.2009.04.015.

[26] Crépin, D., Benomar, Y., Riffault, L., Amine, H., Gertler, A., Taouis, M., 2014. The over-expression of miR-200a in the hypothalamus of ob/ob mice is linked to leptin and insulin signaling impairment. Molecular and Cellular Endocrinology 384(1):1—11. https://doi.org/10.1016/j.mce.2013.12.016.

[27] Derghal, A., Djelloul, M., Airault, C., Pierre, C., Dallaporta, M., Troadec, J.-D., et al., 2015. Leptin is required for hypothalamic regulation of miRNAs targeting POMC 3′UTR. Frontiers in Cellular Neuroscience 9:172. https://doi.org/10.3389/fncel.2015.00172.

[28] Vinnikov, I.A., Hajdukiewicz, K., Reymann, J., Beneke, J., Czajkowski, R., Roth, L.C., et al., 2014. Hypothalamic miR-103 protects from hyperphagic obesity in mice. The Journal of Neuroscience : The Official Journal of the Society for Neuroscience 34(32):10659—10674. https://doi.org/10.1523/JNEUROSCI.4251-13.2014.

[29] Pardini, B., Rosa, F., Naccarati, A., Vymetalkova, V., Ye, Y., Wu, X., et al., 2015. Polymorphisms in microRNA genes as predictors of clinical outcomes in colorectal cancer patients. Carcinogenesis 36(1):82—86. https://doi.org/10.1093/carcin/bgu224.

[30] Ren, Q., Liang, J., Wei, J., Basturk, O., Wang, J., Daniels, G., et al., 2014. Epithelial and stromal expression of miRNAs during prostate cancer progression. American Journal of Translational Research 6(4):329—339.

[31] Santa-Maria, I., Alaniz, M.E., Renwick, N., Cela, C., Fulga, T.A., Van Vactor, D., et al., 2015. Dysregulation of microRNA-219 promotes neurodegeneration through post-transcriptional regulation of tau. The Journal of Clinical Investigation 125(2):681—686. https://doi.org/10.1172/JCI78421.

[32] Pusic, A.D., Kraig, R.P., 2014. Youth and environmental enrichment generate serum exosomes containing miR-219 that promote CNS myelination. Glia 62(2):284—299. https://doi.org/10.1002/glia.22606.

[33] Cheng, H.-Y.M., Papp, J.W., Varlamova, O., Dziema, H., Russell, B., Curfman, J.P., et al., 2007. microRNA modulation of circadian-clock period and entrainment. Neuron 54(5):813—829. https://doi.org/10.1016/j.neuron.2007.05.017.

[34] Nardelli, C., Iaffaldano, L., Ferrigno, M., Labruna, G., Maruotti, G., Quaglia, F., et al., 2013. Characterization and predicted role of the microRNA expression profile in amnion from obese pregnant women. International Journal of Obesity 38:466—469. https://doi.org/10.1038/ijo.2013.121.

[35] Smith, T.H., Sim-Selley, L.J., Selley, D.E., 2010. Cannabinoid CB1 receptor-interacting proteins: novel targets for central nervous system drug

discovery? British Journal of Pharmacology 160(3):454—466 https://doi.org/10.1111/j.1476-5381.2010.00777.x.

[36] Gatta-Cherifi, B., Cota, D., 2015. Endocannabinoids and metabolic disorders. Handbook of Experimental Pharmacology 231:367—391. https://doi.org/10.1007/978-3-319-20825-1_13.

[37] Silvestri, C., Di Marzo, V., 2012. Second generation CB1 receptor blockers and other inhibitors of peripheral endocannabinoid overactivity and the rationale of their use against metabolic disorders. Expert Opinion on Investigational Drugs 21(9):1309—1322. https://doi.org/10.1517/13543784.2012.704019.

[38] Szewczyk, B., Albert, P.R., Rogaeva, A., Fitzgibbon, H., May, W.L., Rajkowska, G., et al., 2010. Decreased expression of Freud-1/CC2D1A, a transcriptional repressor of the 5-HT1A receptor, in the prefrontal cortex of subjects with major depression. The International Journal of Neuropsychopharmacology/Official Scientific Journal of the Collegium Internationale Neuropsychopharmacologicum (CINP) 13(8): 1089—1101. https://doi.org/10.1017/S1461145710000301.

[39] Ou, X.-M., Lemonde, S., Jafar-Nejad, H., Bown, C.D., Goto, A., Rogaeva, A., et al., 2003. Freud-1: a neuronal calcium-regulated repressor of the 5-HT1A receptor gene. The Journal of Neuroscience : The Official Journal of the Society for Neuroscience 23(19):7415—7425.

[40] Collin, M., Bäckberg, M., Onnestam, K., Meister, B., 2002. 5-HT1A receptor immunoreactivity in hypothalamic neurons involved in body weight control. Neuroreport 13(7):945—951.

[41] Vickers, S.P., Dourish, C.T., 2004. Serotonin receptor ligands and the treatment of obesity. Current Opinion in Investigational Drugs (London, England : 2000) 5(4):377—388.

[42] Mancilla-Diaz, J.M., Escartin-Perez, R.E., Lopez-Alonso, V.E., Floran-Garduño, B., Romano-Camacho, J.B., 2005. Role of 5-HT1A and 5-HT1B receptors in the hypophagic effect of 5-HT on the structure of feeding behavior. Medical Science Monitor: International Medical Journal of Experimental and Clinical Research 11(3). BR74-9.

[43] Mato, S., Aso, E., Castro, E., Martín, M., Valverde, O., Maldonado, R., et al., 2007. CB1 knockout mice display impaired functionality of 5-HT1A and 5-HT2A/C receptors. Journal of Neurochemistry 103(5):2111—2120. https://doi.org/10.1111/j.1471-4159.2007.04961.x.

[44] Marco, E.M., Pérez-Alvarez, L., Borcel, E., Rubio, M., Guaza, C., Ambrosio, E., et al., 2004. Involvement of 5-HT1A receptors in behavioural effects of the cannabinoid receptor agonist CP 55,940 in male rats. Behavioural Pharmacology 15(1):21—27.

